Article

TRANSPARENT PROCESS

EMBO reports

Lrig1 is a cell-intrinsic modulator of hippocampal dendrite complexity and BDNF signaling

Fernando Cruz Alsina[1,†], Francisco Javier Hita[1,†], Paula Aldana Fontanet[1], Dolores Irala[1], Håkan Hedman[2], Fernanda Ledda[1] & Gustavo Paratcha[1,*]

Abstract

Even though many extracellular factors have been identified as promoters of general dendritic growth and branching, little is known about the cell-intrinsic modulators that allow neurons to sculpt distinctive patterns of dendrite arborization. Here, we identify Lrig1, a nervous system-enriched LRR protein, as a key physiological regulator of dendrite complexity of hippocampal pyramidal neurons. *Lrig1*-deficient mice display morphological changes in proximal dendrite arborization and defects in social interaction. Specifically, knockdown of *Lrig1* enhances both primary dendrite formation and proximal dendritic branching of hippocampal neurons, two phenotypes that resemble the effect of BDNF on these neurons. In addition, we show that Lrig1 physically interacts with TrkB and attenuates BDNF signaling. Gain and loss of function assays indicate that Lrig1 restricts BDNF-induced dendrite morphology. Together, our findings reveal a novel and essential role of Lrig1 in regulating morphogenic events that shape the hippocampal circuits and establish that the assembly of TrkB with Lrig1 represents a key mechanism for understanding how specific neuronal populations expand the repertoire of responses to BDNF during brain development.

Keywords dendrite morphogenesis; hippocampal neurons; Lrig1; neurotrophins; TrkB

Subject Categories Cell Adhesion, Polarity & Cytoskeleton; Neuroscience; Signal Transduction

DOI 10.15252/embr.201541218 | Received 19 August 2015 | Revised 26 January 2016 | Accepted 28 January 2016 | Published online 2 March 2016

EMBO Reports (2016) 17: 601–616

Introduction

Dendritic tree complexity, which results from the interplay between extrinsic factors, cell type specific signaling modulators, and electrical activity, can regulate the transmission of information in the nervous system [1,2]. Throughout development, several extrinsic factors control dendritic growth and branching activating specific signaling pathways that affect the cytoskeleton and gene expression [3]. Neurotrophins are a structurally related group of extracellular factors represented by nerve growth factor (NGF), brain-derived neurotrophic factor (BDNF), neurotrophin 3 (NT3), and neurotrophin 4/5. They play critical roles during neuronal development supporting survival, axonal and dendritic growth, guidance, branching, and neuronal plasticity of specific populations of sensory, sympathetic, and central nervous system (CNS) neurons, via the activation of their cell-surface receptor tyrosine kinases, tropomyosin-related kinase (Trk) A (TrkA), TrkB, and TrkC [4]. BDNF is one of the most studied extrinsic factors that regulate growth, branch morphology, and spine density of developing dendrites [5–10]. In hippocampal and cortical pyramidal neurons, BDNF increases the number of primary dendrites and dendrite branches near the cell body [7,11–14].

Recent studies provide compelling evidence that transmembrane proteins containing extracellular leucine-rich repeat (LRR) domains control neuronal connectivity functioning as regulators of axon guidance, dendritic growth, synapse formation, and plasticity [15–17]. Distinct LRR protein families are highly enriched in the CNS, especially in the hippocampus, where they play a critical role in organizing synaptic connections into functional neural circuits. Given their crucial role in the organization of neuronal connectivity, it seems likely that dysfunctions in LRR genes or in their binding partners could compromise neuronal function and lead to neurodevelopmental and neuropsychiatric disorders [18].

In particular, leucine-rich repeats and immunoglobulin (Ig)-like domains 1 (Lrig1) is a transmembrane protein highly expressed in the CNS that contains 15 LRRs and 3 Ig domains in its extracellular region [19,20]. Previous research points to Lrig1 as a receptor tyrosine kinase (RTK)-associated protein able to regulate neurotrophic growth factor receptor signaling [21–24]. Interestingly, neurotrophic factor-induced RTK signaling is required for proper nervous system development and plasticity, and abnormalities in the control of this signaling have been associated with diverse brain disorders and tumors [25,26].

While the specific roles of many LRR integral proteins have recently been addressed [15], the physiological contribution of

1 Division of Molecular and Cellular Neuroscience, Institute of Cell Biology and Neuroscience (IBCN)-CONICET, School of Medicine, University of Buenos Aires (UBA), Buenos Aires, Argentina
2 Oncology Research Laboratory, Department of Radiation Sciences, Umeå University, Umeå, Sweden
*Corresponding author. Tel: +54 11 5950-9500; Fax: +54 11 5950-9626; E-mails: gparatcha@fmed.uba.ar or gustavo.paratcha@conicet.gov.ar
†These authors contributed equally to this study

Lrig1 for brain development remains to be determined. In the present work, we explore the role of Lrig1 in developing hippocampal neurons by first studying the expression pattern of Lrig1 during hippocampal development. The prominent expression of Lrig1 at the moment that hippocampal dendrite development takes place, prompted us to examine whether Lrig1 could regulate dendritogenesis and dendritic tree arborization of hippocampal neurons.

In the current study, we describe novel functions for Lrig1 as an endogenous inhibitor of hippocampal dendrite morphogenesis and branching. Our data also establish Lrig1 as an essential molecule linking TrkB signaling to dendrite development and suggest that Lrig1 contributes to shape distinctive patterns of dendritic arborization in specific neuronal populations in response to neurotrophins. Furthermore, loss of Lrig1 led not only to morphological abnormalities but also to social behavior deficits, highlighting the importance of this cell-intrinsic modulator for normal nervous system development and plasticity.

Results

Expression of Lrig1 during hippocampal development

Although specific roles for many LRR proteins have recently been uncovered in connectivity and synapse formation in forebrain neurons, the role of Lrig1 in nervous system development is still unclear. To address this, the expression of *Lrig1* mRNA was analyzed by real-time RT–PCR in rat hippocampal tissue at different developmental stages (Fig 1A). An increase in *Lrig1* mRNA expression was detected during the first and second postnatal weeks, the main period of hippocampal dendrite development and synaptogenesis in rodents. This increase was detected between postnatal day 0 (P0) and P15, with a peak of expression at P15.

To determine which cell types express Lrig1, we examined the localization of Lrig1 in brain sections containing the hippocampus. Immunofluorescence of tissue sections obtained from 2-week-old rats revealed that Lrig1 is highly expressed in dentate granule cells and pyramidal neurons in the cortex and in CA1–CA3 hippocampal areas (Fig 1B–E). Interestingly, Lrig1 staining mainly concentrates in the soma and extends out into the apical dendrites of CA1–CA3 hippocampal (Fig 1D and E) and cortical pyramidal neurons (Fig 1C). As expected, no signal for Lrig1 expression could be detected neither in sections of CA1 hippocampal pyramidal neurons nor in hippocampal lysates obtained from Lrig1-mutant mice (Fig EV1A and B). In addition, specific detection of mouse Lrig1 by immunofluorescence was controlled by downregulation of endogenous Lrig1 expression in hippocampal primary neurons transfected with *Lrig1*-shRNA (Fig EV2A and B) and immunoblot containing cell extracts overexpressing each Lrig-family member (Fig EV1C).

Dissociated hippocampal cultures show that virtually all neurons (βIII-tubulin$^+$), but not astrocytes (S100β^+), were found to express Lrig1 (Fig 1F and G). In mature primary hippocampal neurons, Lrig1 immunoreactivity is mainly localized to both cell bodies and proximal neuritic processes co-stained with the dendritic marker MAP-2 (Fig 1H).

Knockdown of Lrig1 promotes dendritic development of hippocampal neurons

To determine whether Lrig1 could regulate dendrite patterning, we used a plasmid-based shRNA interference system to knockdown Lrig1 expression in cultured neurons. In a previous work, we have identified a shRNA-targeted sequence in mouse *Lrig1* mRNA (nt 1494–1512) that specifically reduces Lrig1 expression levels in cultured cells [24]. Here, we additionally controlled the efficiency of our shRNA construct by real-time RT–PCR (Fig 2H), immunoblotting, and immunofluorescence of transfected hippocampal neurons (Fig EV2).

To evaluate the involvement of Lrig1 in dendritic development, P0 mouse dissociated hippocampal neurons maintained for 9 days *in vitro* (9 DIV) were transfected with a GFP-expressing control plasmid or *Lrig1*-shRNA-GFP-expressing vector. Three days after transfection (12 DIV), the neurons were fixed and analyzed. Dendritic complexity was determined using Sholl analysis, which measures the number of times that dendrites pass across concentric circles localized at different distances from the cell bodies [27]. Using this analysis, we found that knockdown of *Lrig1* in primary hippocampal neurons leads to a significant increase in their proximal dendritic tree arborization, particularly within the ~90 μm closest to the soma (Fig 2A and B). Consistent with this result, we also observed that *Lrig1* knockdown caused a significant increase in various dendritic parameters such as the number of primary and secondary dendrites, total dendritic growth, and branching (Fig 2C-G).

We also analyzed neurons cultured from *Lrig1*$^{+/+}$ and *Lrig1*$^{-/-}$ mice. Similar dendritic changes were observed when we compared wild-type (wt) vs. *Lrig1*-deficient neurons cultured for 7 DIV and stained with the dendritic marker MAP-2 (Fig 2I). Using Sholl analysis, we found that cultured hippocampal neurons from P0 *Lrig1*-null mice exhibited higher proximal dendritic tree complexity than wild-type control neurons (Fig 2J). This dendritic complexity resulted from a significant enhancement in the branching, in the number of secondary dendrites and in the number of dendrites directly extending from the neuronal cell body, confirming our results from shRNA experiments (Fig 2K–M).

The increased dendrite complexity of *Lrig1*-deficient neurons was additionally detected at different *in vitro* developmental stages (e.g., at 7, 10, and 14 DIV). The changes in total dendritic length and branching were stronger as neurons become more mature (Fig EV3). Immunoblot analysis confirmed the complete absence of Lrig1 protein in the hippocampus of *Lrig1*-knockout mice (Fig EV1B).

Loss of Lrig1 leads to enhanced apical dendrite arborization of CA1–CA3 pyramidal neurons *in vivo*

To determine whether the data obtained from cultured neurons have *in vivo* relevance, we evaluated dendritic arborization of hippocampal CA1 and CA3 pyramidal neurons in *Lrig1*-knockout mice. Abnormalities in dendrite morphogenesis observed in hippocampal neurons *in vitro* were corroborated by Golgi-stained dendritic arbors *in vivo* (Fig 3). Proximal branching and the number of primary dendrites in CA1 hippocampal pyramidal neurons were

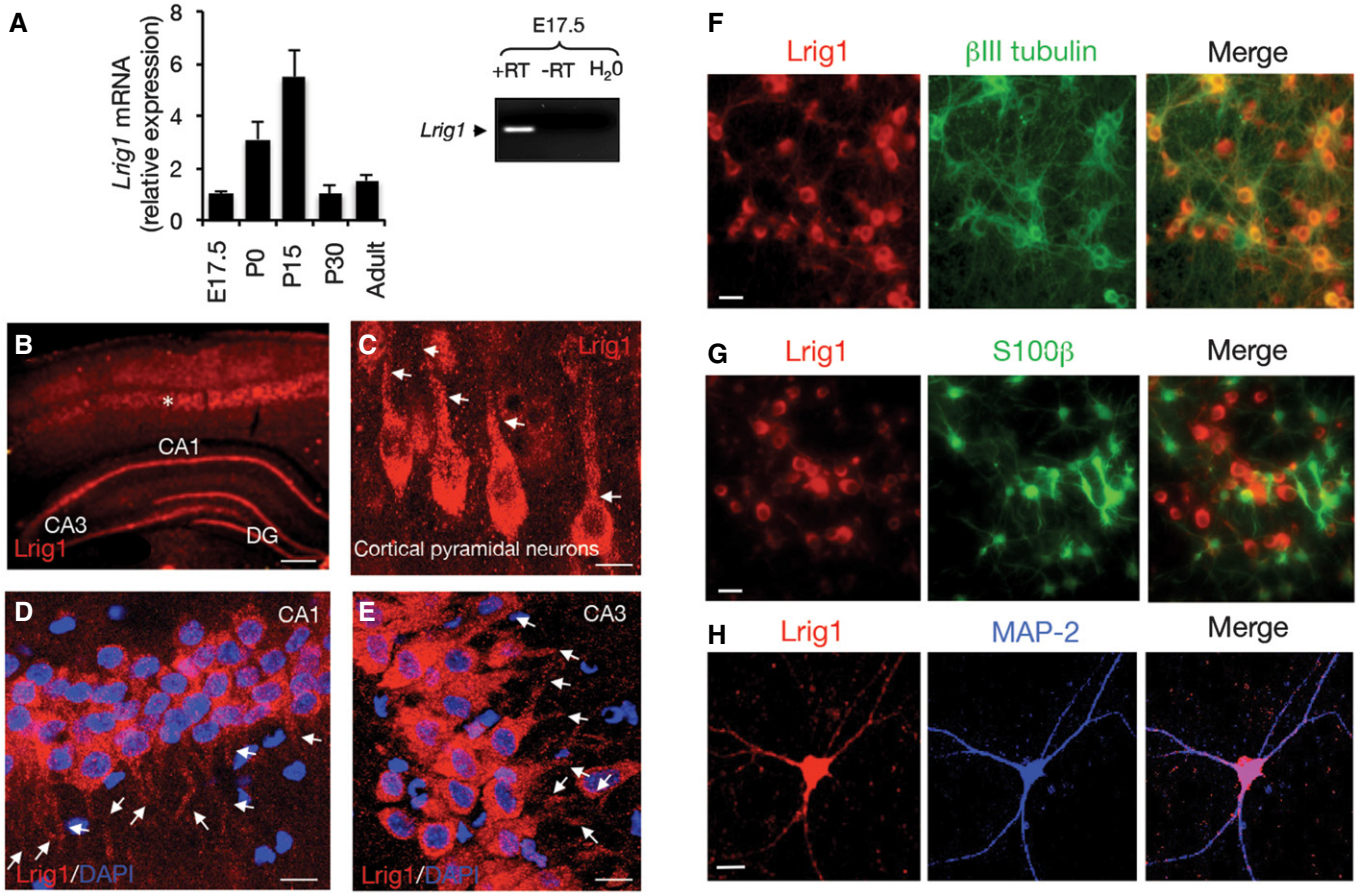

Figure 1. Developmental expression and somatodendritic localization of Lrig1 in hippocampal neurons.

A Quantitative analysis of developmental expression of *Lrig1* mRNA in rat hippocampus by real-time RT–PCR. The results are shown as mean ± SEM of $n = 3$ independent assays. The levels of *Lrig1* mRNA were normalized using the expression of the housekeeping gene *Tbp* (TATA box-binding protein). The insert shows the expression of Lrig1 in embryonic E17.5 rat hippocampus examined by RT–PCR. Control sample without reverse transcriptase (-RT) is also shown.

B Localization of Lrig1 (red) in coronal sections from P15 rat brain by immunofluorescence. Anti-Lrig1^{ECD} antibodies label dentate gyrus cells, CA1–CA3 hippocampal neurons, and pyramidal cortical neurons (asterisk). Scale bar, 400 μm.

C–E Confocal image of cortical (C) and hippocampal (D, E) pyramidal neurons stained with rabbit anti-Lrig1^{ECD} antibody. Arrows indicate Lrig1 staining in proximal segments of apical dendrites of CA1–CA3 hippocampal and pyramidal cortical neurons (layer V). Scale bars, 20 μm.

F Immunofluorescence staining of Lrig1 (red) with anti-Lrig1^{ECD} antibody and the neuronal marker βIII-tubulin (green) in dissociated hippocampal cells cultured for 7 DIV. Yellow indicates neuronal expression of Lrig1. Scale bar, 15 μm.

G Immunofluorescence staining of Lrig1 (red) with anti-Lrig1^{ECD} antibody and the astrocytic marker S100β (green) in dissociated hippocampal cells cultured for 7 DIV. Scale bar, 20 μm.

H Localization of Lrig1 (red) with anti-Lrig1^{ECD} antibody and the somatodendritic marker MAP-2 (blue) by immunocytochemistry in dissociated rat hippocampal neurons after 12 DIV. Scale bar, 20 μm.

Data information: All data represent at least three independent experiments.

significantly increased in *Lrig1*-null mice compared to littermate controls at 4–5 weeks of postnatal age (Fig 3A and B). Moreover, total dendrite intersections obtained by Sholl analysis demonstrated significant differences in proximal dendritic arborization of CA1 hippocampal neurons (Fig 3C), characterized by a higher complexity in the apical than in the basal dendritic domain (Fig 3D). Dendritic branching was also markedly enhanced in apical dendrites of CA1 hippocampal neurons, further supporting a preferential apical dendrite phenotype in *Lrig1*-null mice (Fig 3B). Similar results were also obtained in hippocampal CA3 pyramidal neurons (Fig EV4).

Lrig1-knockout mice display social behavior abnormalities

Structural abnormalities of dendrites and their connections are related to impaired sociability and dysregulated social behavior [28–30]. As previously shown in Fig 1, Lrig1 is highly expressed in the hippocampus, a brain area that among many other behaviors has also been implicated in sociability [31,32]. Due to the fact that *Lrig1*-deficient mice tended to be isolated from their littermates within the cage, we decided to examine whether *Lrig1*-mutant mice display altered social behaviors. To measure social interaction, wild-type and knockout mice were subjected to a three-chamber

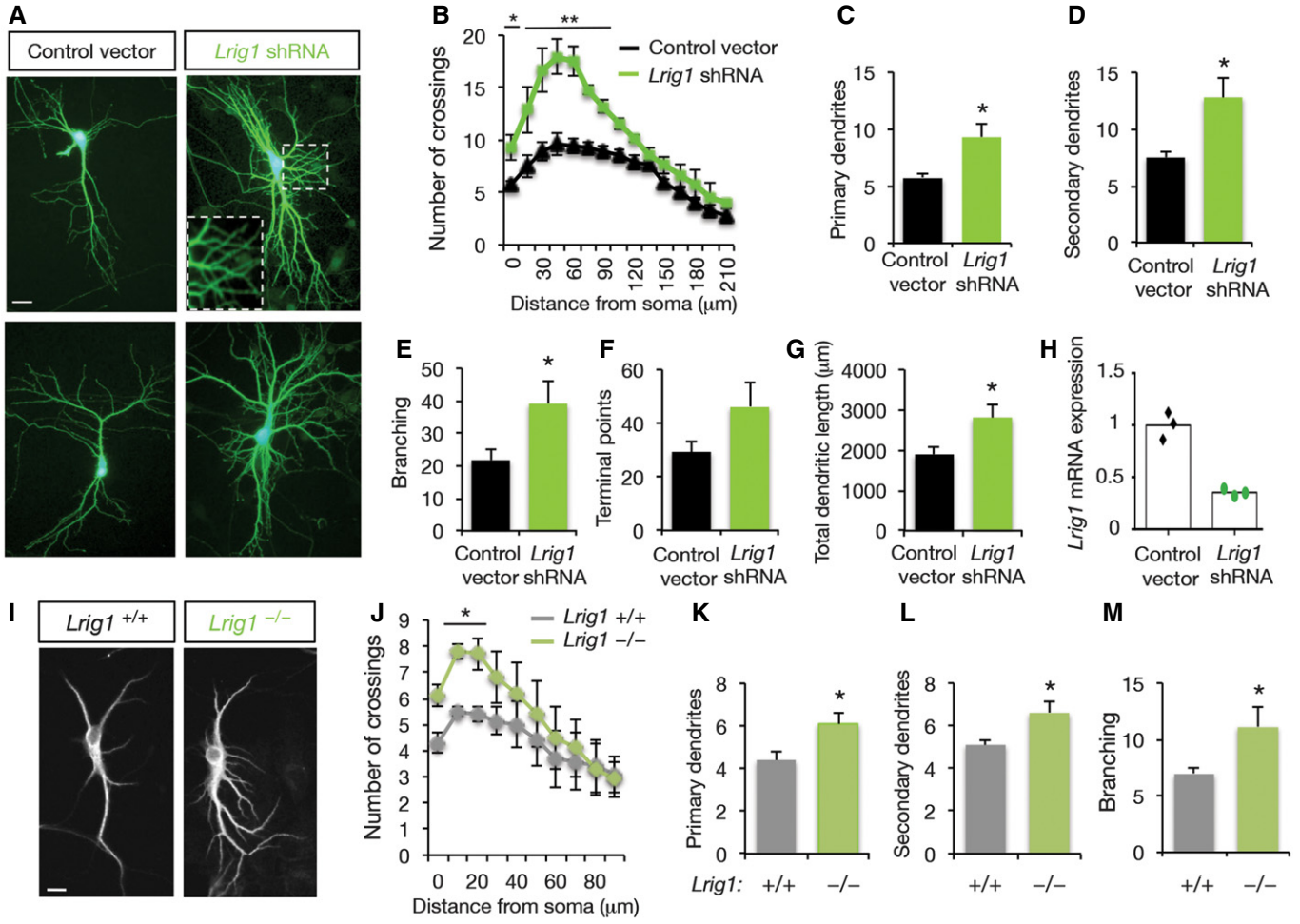

Figure 2. Lrig1 downregulation potentiates dendritic growth and branching of hippocampal neurons.

A Representative images of mouse hippocampal neurons transfected with either GFP-expressing control or *Lrig1*-shRNA vector at 9 DIV and maintained for 3 additional days *in vitro* (9 + 3 DIV). Scale bar, 15 μm. Boxed area represents a higher magnification image showing the profuse proximal dendritic arborization of *Lrig1*-shRNA-transfected neurons.

B Sholl analysis of the dendritic arbor from hippocampal neurons transfected with either control or *Lrig1*-shRNA-GFP vector at 9 DIV and maintained for 3 additional days *in vitro* (9 + 3 DIV). Data are shown as mean ± SEM of $n = 3$ independent experiments. *$P < 0.05$ and **$P < 0.01$ by two-way ANOVA followed by Bonferroni multiple comparisons test.

C–G Quantification of primary (C) and secondary (D) dendrites as well as total dendritic branching (E), terminal dendritic points (F), and total dendritic length (G) of hippocampal neurons transfected with either control or *Lrig1*-shRNA-GFP vector. The results are shown as mean ± SEM of $n = 3$ independent experiments. *$P < 0.05$ by Student's *t*-test.

H Knockdown efficiency was analyzed by real-time RT–PCR in MN1 cells transfected with control or *Lrig1*-shRNA vectors. Transfected cells were enriched by puromycin treatment in order to increase the population of cells expressing control or *Lrig1*-shRNA constructs. Data are shown as individual values of a representative assay measured in triplicates. $n = 2$ independent experiments were performed.

I Representative images of MAP-2 immunostained hippocampal neurons obtained from wild-type and Lrig1-deficient mice cultured for 7 days *in vitro* (7 DIV). Scale bar, 15 μm.

J Sholl analysis of the dendritic arbor from MAP-2 stained hippocampal neurons (7 DIV) isolated from wild-type and *Lrig1*-deficient mice. Data are shown as mean ± SEM of $n = 3$ independent experiments. *$P < 0.05$ by two-way ANOVA followed by Bonferroni multiple comparisons test.

K–M Quantification of the number of primary dendrites (K), secondary dendrites (L), and total dendritic branching (M) from MAP-2 stained hippocampal neurons (7 DIV) isolated from wild-type and *Lrig1*-deficient mice. The results are shown as mean ± SEM of $n = 3$ independent experiments. *$P < 0.05$ by Student's *t*-test.

Data information: Note that the different scales of values obtained between shRNA-mediated knockdown and knockout neurons (panels B and J) are due to differences in the experimental conditions between both assays (densities of the cultures and days that the cells were maintained in culture).

social interaction test. After habituation, mice were allowed to choose between a chamber containing a caged age-matched conspecific mouse (stranger 1) and a chamber containing an empty container (Fig 4A). As expected, control wt mice exposed to a novel conspecific juvenile exhibited typical behavior of approaching and sniffing, but such a social motivation and interaction were profoundly decreased in *Lrig1*-mutant mice (Fig 4B and C). Subsequently, when mice were exposed to the familiar mouse versus a novel mouse (stranger 2), wt control mice showed a clear preference for the novel mouse over the familiar one, while knockout

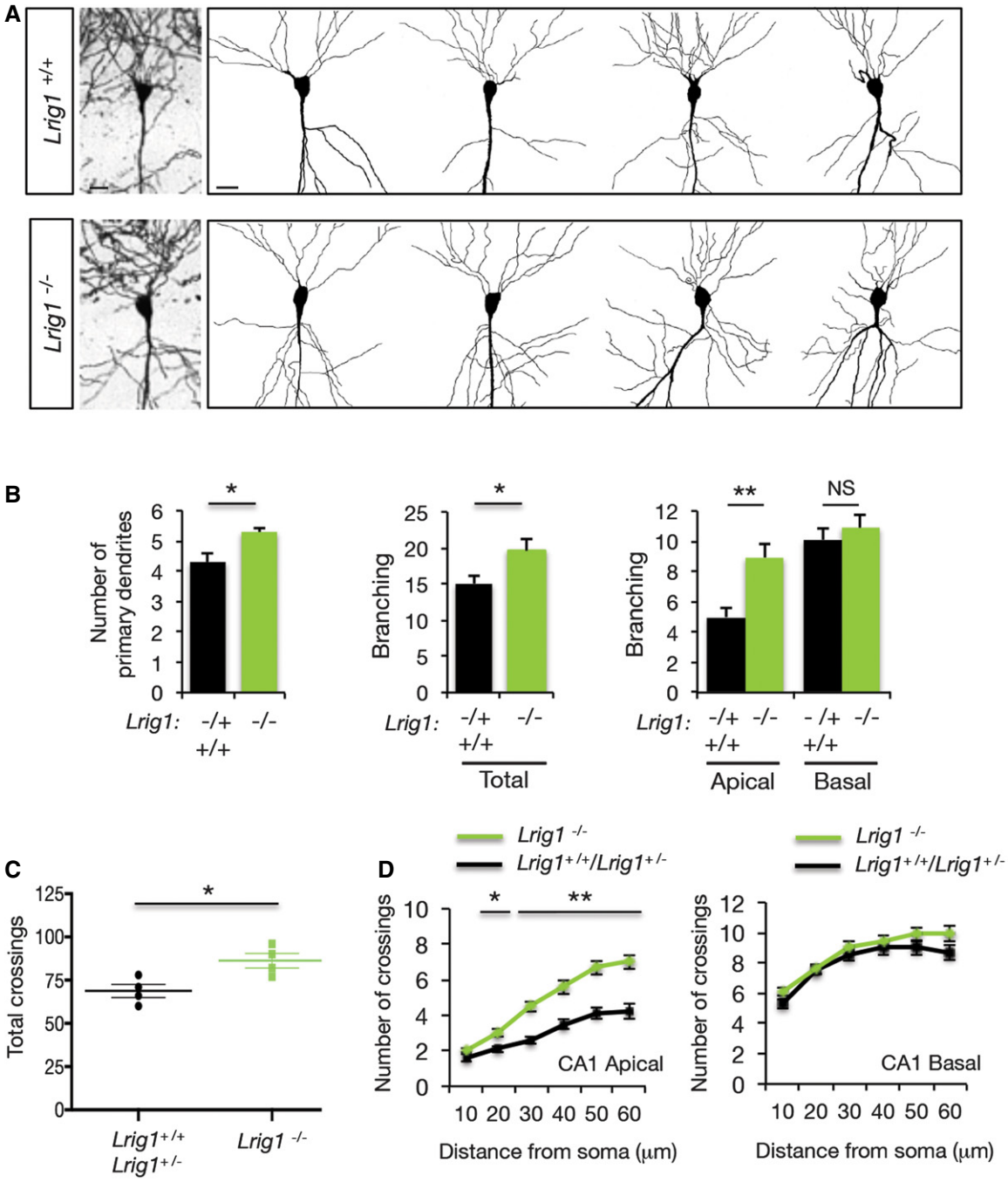

Figure 3. Lrig1 controls apical dendrite arborization of CA1 pyramidal neurons.

A Representative images and drawings of Golgi-stained hippocampal CA1 pyramidal neurons from 4-week-old wild-type and *Lrig1*-null littermate mice. Scale bar, 15 μm.

B Quantification of the number of primary dendrites and branching of apical and basal dendritic arbors of hippocampal CA1 pyramidal neurons from 4- to 5-week-old control (wild-type/heterozygous) and *Lrig1*-null littermate mice. The results are shown as mean ± SEM of independent determinations performed in $n = 4$ mice of each genotype. *$P < 0.05$, **$P < 0.001$ by Student's *t*-test. NS, not significant.

C Cumulative dendrite crossings of concentric circles of increasing radius (10 μm ring interval) centering the reference point at the cell body. These values were obtained by Sholl analysis and represent the summatory of the dendritic crossings registered within the first 60 μm closest to the soma. The results are shown as mean ± SEM of independent determinations performed in $n = 4$ mice of each genotype. *$P < 0.05$ by Student's *t*-test.

D Sholl analysis of apical and basal dendritic arbors of hippocampal CA1 pyramidal neurons from 4- to 5-week-old control (wild-type/heterozygous) and *Lrig1*-null littermate mice. The results are shown as mean ± SEM. *$P < 0.05$, **$P < 0.001$ by two-way ANOVA followed by Bonferroni multiple comparisons test.

Data information: Quantifications shown in (B–D) were performed in $n = 60$ neurons from 4 wild-type/heterozygous mice and 4 *Lrig1*-null littermate mice ($n = 4$).

mice did not show a significant preference for social novelty (Fig 4D and E). In addition, mutant mice displayed significantly less interaction with the novel target mouse compared to controls. Thus, the *Lrig1*-mutant mice behaviorally display social interaction deficits that correlate with alterations in dendrite arborization of CA1–CA3 hippocampal neurons.

Lrig1 overexpression reduces hippocampal dendritogenesis and dendritic spine number in response to BDNF

Previous reports established that BDNF and its receptor TrkB induce proximal dendritic complexity mainly characterized by an enhancement in the amount of primary and secondary dendrites and in spine density of hippocampal developing neurons [9,12–14]. On the other hand, Lrig1 is a receptor tyrosine kinase-associated protein that regulates multiple growth factor receptor signaling pathways [25]. Therefore, these observations prompted us to investigate whether the increase in dendritic complexity observed upon downregulation of Lrig1 expression in hippocampal neurons could be the result of enhanced responsiveness to BDNF.

To study the role of Lrig1 on BDNF-mediated dendrite development, we performed gain of function assays overexpressing Lrig1 in cultured hippocampal neurons. For this purpose, dissociated hippocampal neurons were transfected at 7 DIV with control (empty vector) or Flag-tagged Lrig1 plasmids in combination with an enhanced green fluorescent protein (GFP) expression vector. After transfection, neurons were cultured in the absence or in the presence of BDNF for 72 h, and analyzed at 10 DIV for dendrite development. In agreement with previous reports, we found that BDNF enhances the number of primary and secondary dendrites in hippocampal neurons transfected with a control vector. However, BDNF failed to promote morphological dendritic changes in hippocampal neurons overexpressing a cDNA encoding full-length (FL) Flag-tagged Lrig1 (Fig 5A–D). To identify which domain of Lrig1 is required for this inhibitory effect, we overexpressed mutants of Lrig1 either lacking both LRR and Ig domains (ΔLRRIg) or lacking the LRR domain (ΔLRR). Unlike full-length Lrig1, both mutated forms of Lrig1 lose their ability to block the formation of primary and secondary dendrites in response to BDNF (Fig 5B–D). Together, these findings demonstrate that Lrig1 LRR domain is required for the inhibitory function of Lrig1 on BDNF activity. Ectopic expression of these Flag-tagged Lrig1 mutants is shown in Fig 5A.

In addition to restrict the formation of primary and secondary dendrites, Lrig1 overexpression also blocked BDNF-induced dendritic spine density in primary hippocampal neurons (Fig 5E and F), supporting the role of Lrig1 as an endogenous inhibitor of BDNF-promoted hippocampal dendrite development.

Lrig1 interacts with TrkB, regulates neurotrophin-induced receptor activation, and its expression is induced in hippocampal neurons by BDNF

Notably, the *in vivo* localization observed for Lrig1 in hippocampal sections (Fig 1B) is consistent with the previously described expression pattern of TrkB in CA1–CA3 pyramidal neurons and dentate gyrus granule cell layer [33–35]. As reported previously, *in vitro* immunostainings revealed that TrkB is expressed in almost all cultured hippocampal neurons and is primarily localized in somata and dendrites [36]. Our findings indicate that more than 95% of the $TrkB^+$ neurons coexpressed Lrig1, and that both proteins are highly colocalized in the somatodendritic compartment *in vitro* (Fig 6A). Thus, this evidence additionally supports a role of Lrig1 in the control of TrkB receptor signaling.

Previous studies revealed the importance of negative feedback control of receptor function as a mechanism to ensure signaling thresholds compatible with the induction of a physiological response [25,37,38]. Based on this concept, we analyzed whether Lrig1 gene expression could be induced after BDNF treatment of hippocampal neurons. Real-time RT–PCR analysis revealed a significant induction of *Lrig1* mRNA after stimulation of hippocampal primary neuronal cultures with BDNF (Fig 6B).

Next, we examined the possibility that Lrig1 may interact physically with TrkB receptor. To address this possibility, HEK293 cells were transfected with expression vectors encoding the HA-tagged TrkB receptor in the absence or presence of Flag-tagged Lrig1, and then, Lrig1 was immunoprecipitated with anti-Flag antibodies. As shown in Fig 6C, TrkB was specifically coimmunoprecipitated with anti-Flag antibodies only from cells coexpressing both constructs, but not from cells transfected with control or each construct alone, indicating that Lrig1 interacts with TrkB. This interaction was additionally confirmed pulling-down TrkB with pan-Trk antibodies followed by immunoblotting with anti-Flag (Fig 6E). This interaction is specific, as it was not observed for other Lrig members (Lrig2 and Lrig3) (Fig 6D and E), or for the other neurotrophin receptor TrkA [24].

To determine whether the interaction between Lrig1 and TrkB receptor occurs when these proteins are expressed at physiological levels, Lrig1 was immunoprecipitated from tissue extracts prepared from P15 rat hippocampi. These assays revealed that TrkB can be coimmunoprecipitated with Lrig1, but not with control antibodies (Fig 6F), demonstrating that Lrig1 and the TrkB receptor specifically associate in the brain.

To investigate whether Lrig1 might regulate TrkB neurotrophin receptor activation, HEK cells were transfected to overexpress HA-tagged TrkB in the presence or in the absence of Flag-tagged Lrig1. Then, cells were serum-starved and treated with or without BDNF for 15 min. TrkB activity was assessed by probing cell lysates with a specific antibody that recognizes the phosphorylated form of TrkB in tyrosine 705 (Y705), a tyrosine placed within the activation loop of TrkB kinase domain. Interestingly, cells expressing Lrig1 showed a substantial reduction in BDNF-induced TrkB phosphorylation (Fig 6G), indicating that Lrig1 interacts with TrkB to inhibit receptor activation and BDNF signaling. The ability of Lrig1 to regulate TrkB was additionally explored by neurite growth assays of PC12 cells expressing HA-TrkB either in the presence or in the absence of Flag-tagged Lrig1. Ectopic expression of Lrig1 in PC12 cells expressing HA-TrkB reduces neurite outgrowth activity in response to BDNF (Fig EV5).

Previous works have demonstrated that Lrig1 restricts ErbB and Met receptor signaling by enhancing receptor ubiquitination and degradation [21–23]. Therefore, we further examined whether Lrig1 could promote the ubiquitination and degradation of TrkB in cells treated with MG-132, a potent and highly specific

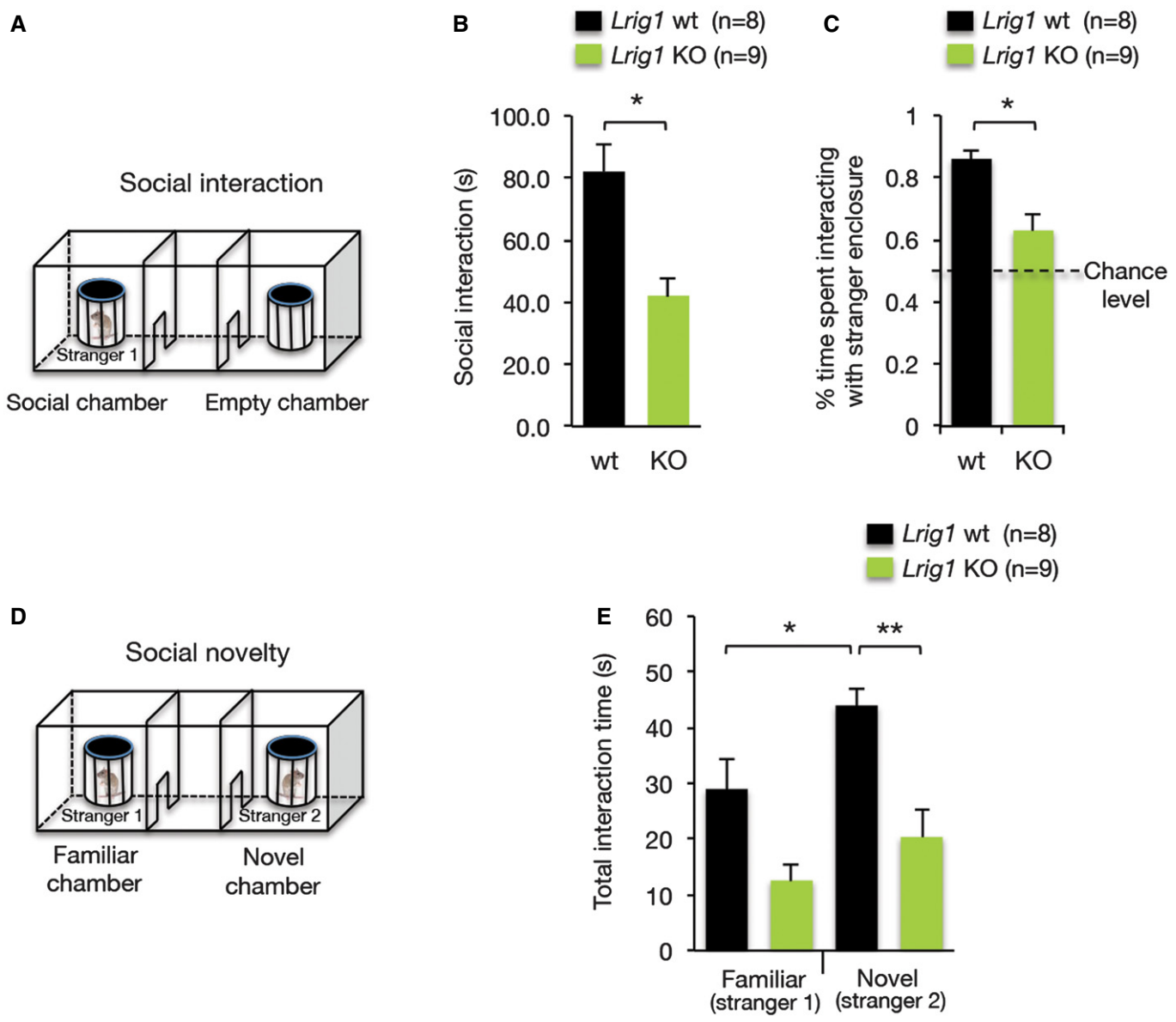

Figure 4. *Lrig1* knockout mice exhibit social interaction impairments.

A Schematic diagram of the social interaction device indicating the social and the empty chambers.

B, C Mice were simultaneously exposed to an empty container and a caged unfamiliar juvenile mouse (social enclosure, stranger 1). *Lrig1*-mutant mice exhibit social interaction defects as determined by the time spent interacting (sniffing) with the stranger enclosure (B) and the percentage of total interaction time with stranger in the three-chamber social interaction test (C). Dashed line in (C) represents chance-level performance (i.e., 50%) when mice equally explore the social enclosure and the empty container. Data represent means ± SEM of independent determinations performed in n = 8–9 mice of each genotype, and the statistical significance between wt and knockout mice is $^*P < 0.05$ by Student's t-test.

D Schematic diagram of the social novelty test. In the test for social novelty, a second stranger (stranger 2) mouse was introduced in the empty container.

E In the preference for social novelty task, wt mice showed a preference for social novelty, while mutant mice showed no significant preference for novel target (stranger 2). Mutants also spent significantly less time interacting with the novel mice compared to controls. Data represent means ± SEM of independent determinations performed in n = 8–9 mice of each genotype, and the statistical significance is as follows: $^*P < 0.05$ and $^{**}P < 0.005$ by ANOVA followed by Student–Newman–Keuls' multiple comparisons test.

proteasome inhibitor, before stimulation with BDNF. An increased ubiquitination of TrkB was clearly associated with its activation level (Fig 6H). Thus, ectopic expression of Lrig1 resulted in a reduced TrkB activation and ubiquitination. These results are in contrast with a role of Lrig1 in the promotion of TrkB degradation by ubiquitination, and suggest that in this case the poor ubiquitination of TrkB is a consequence of the reduced activation of the receptor and not the cause. In conclusion, these data indicate that TrkB inhibition by Lrig1 is not associated with receptor ubiquitination and degradation.

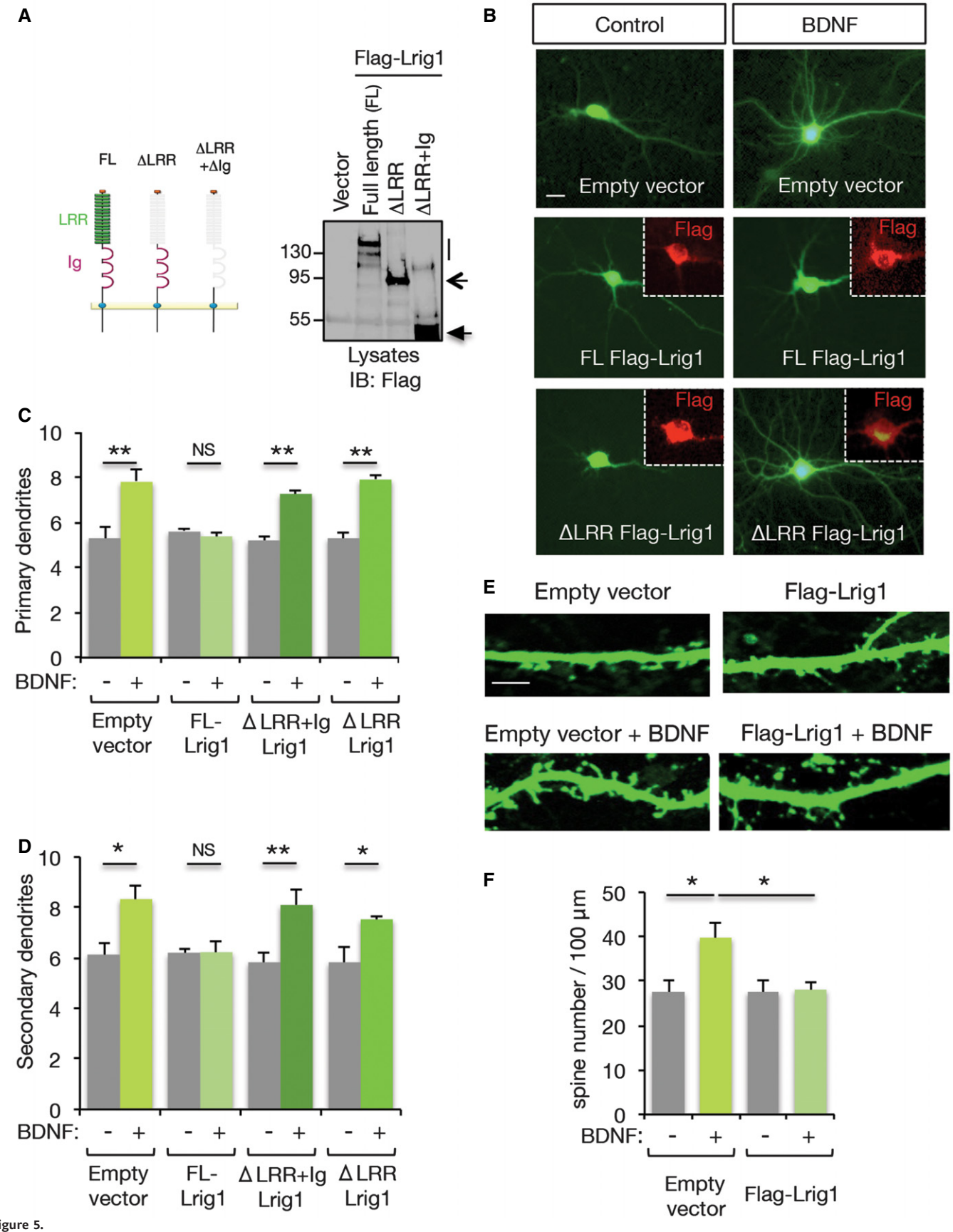

Figure 5.

Figure 5. Lrig1 overexpression restricts hippocampal dendrite morphology and dendritic spine density in response to BDNF.

A Schematic representation of Lrig1 mutants is shown on the left. Expression levels of these mutants were analyzed in transfected cell extracts by immunoblotting with anti-Flag antibodies.

B Representative images of rat hippocampal neurons transfected at DIV8 with empty vector, full-length (FL) Flag-tagged Lrig1, or Lrig1 mutant lacking the LRR domain (ΔLRR) in combination with an enhanced green fluorescent protein (GFP) expression vector. After transfection at 9 DIV, neurons were cultured in the absence or in the presence of BDNF (30 ng/ml) for 48 h. Then, hippocampal cultures at 11 DIV were fixed and stained with anti-Flag antibodies to control Lrig1 expression. Scale bar, 15 μm.

C, D Quantification of the effects of Flag-Lrig1 constructs on BDNF-induced primary (C) and secondary (D) dendrite formation of hippocampal neurons treated as indicated in (A). The results are shown as mean ± SEM of 3 independent experiments. $*P < 0.05$, $**P < 0.01$ by one-way ANOVA followed by Tukey's multiple comparisons test. NS, not significant.

E Representative confocal images of dendritic shafts containing spines from hippocampal neurons transfected at 15 DIV with either control vector or Flag-Lrig1 construct together with GFP. After transfection, neurons were cultured in the absence or in the presence of BDNF (30 ng/ml) for 48 h (15 + 3 DIV). Scale bar, 5 μm.

F Quantification of the effect of Lrig1 overexpression on neurotrophin-induced spine density. The results are shown as mean ± SEM of $n = 3$ independent experiments. $*P < 0.05$ by one-way ANOVA followed by Student–Newman–Keuls' multiple comparisons test.

Downregulation of Lrig1 enhances TrkB signaling and dendrite development of hippocampal neurons in responses to BDNF

In order to analyze whether Lrig1 affects BDNF-dependent TrkB signaling, we examined TrkB phosphorylation and its downstream effector MAPK in hippocampal cultures from *Lrig1*-knockout ($Lrig1^{-/-}$) and wt ($Lrig1^{+/+}$) mice treated with BDNF. Consistent with a role of Lrig1 in the control of TrkB function, a significant potentiation of both BDNF-induced TrkB tyrosine phosphorylation (Fig 7A and B) and MAPK activation (Fig 7C and D) was observed when *Lrig1*-deficient hippocampal neurons were compared to wt neuronal cultures.

Next, we decided to analyze whether Lrig1 downregulation affects biological responses of hippocampal neurons to BDNF. In agreement with a role of Lrig1 as a negative regulator of neurotrophin-induced TrkB activation, a substantial increase of dendrite development was observed in those hippocampal neuronal cultures transfected at 4 DIV with *Lrig1*-shRNA and stimulated with BDNF for 72 h (4 + 3 DIV) (Fig 7E). Notably, dendritic branching as well as the number of primary and secondary dendrites of hippocampal neurons was markedly increased in *Lrig1*-shRNA-expressing neurons treated with BDNF (Fig 7F–H). In particular, a greater number of short neurites arising from the principal dendrite of *Lrig1*-shRNA-transfected neurons was also observed in the presence of BDNF (Fig 7I). This biological response is consistent with the high complexity observed in the apical dendrite domain of *Lrig1* knockout pyramidal neurons *in vivo*. These results demonstrate a potentiation of the dendritogenic effects of BDNF in *Lrig1*-deficient neurons. To further explore the involvement of Lrig1 in the control of TrkB activation *in vivo*, the levels of p-Tyr705 TrkB in $Lrig1^{+/+}$ and $Lrig1^{-/-}$ hippocampal lysates were examined. In agreement with a role of Lrig1 as a physiological regulator of TrkB, a substantial increase in TrkB phosphorylation was observed in $Lrig1^{-/-}$ hippocampal lysates compared to samples prepared from $Lrig1^{+/+}$ mice (Fig 7J). Taken together, these findings provide evidence of a novel regulatory mechanism that permit a precise refinement of hippocampal dendrite arborization in response to BDNF.

Discussion

How neurons develop their dendritic morphologies is a crucial question in neurobiology. In this study, we found that Lrig1 is an intrinsic suppressor of hippocampal dendrite morphogenesis and branching. Furthermore, our data are consistent with a role of Lrig1 as a negative regulator of BDNF signaling and TrkB-mediated dendritic development. Several lines of evidence support these findings. First, Lrig1 binds to TrkB and TrkB signaling is enhanced in *Lrig1*-deficient hippocampal neurons treated with BDNF. Second, knockdown of *Lrig1* increases dendrite formation and branching induced by BDNF. Third, overexpression of full-length Lrig1 in hippocampal neurons blocks both primary dendrite formation and reduces spine density in response to BDNF, indicating that Lrig1 restricts TrkB function associated to dendrite development.

Extensive evidence implicates the actions of several extrinsic and intrinsic factors in dendrite arborization. In particular, the cell-intrinsic control of dendrite morphology is a key mechanism that coordinates the timing of dendrite morphogenesis and the specificity of dendrite patterning. During development, different neuronal domains encounter similar environmental factors. However, intrinsic modulators of these pathways, located within specific domains of the neurons, control the cellular interpretation of these extrinsic cues, thereby allowing neurons to generate distinct patterns of dendritic arborization [39]. Little is known about the molecular mechanisms that direct morphogenesis and complexity of specific dendritic domains within the same dendritic arbor [30]. Our *in vivo* analyses demonstrate that Lrig1 ablation preferentially increases the proximal complexity of the apical dendrites of hippocampal CA1–CA3 pyramidal neurons. Therefore, our work also contributes to the understanding of the molecular mechanisms involved in basal versus apical dendrite morphogenesis during pyramidal neuron development in the hippocampus.

Dendrite morphology is a key determinant of the functional properties of neurons, and many neurodevelopmental and psychiatric disorders are due primarily to structural abnormalities of dendrites and their connections [28,29]. For example, mental retardation and autism spectrum disorders are genetic diseases often associated with overgrowth or lack of dendrite pruning during development, and characterized by impaired sociability and dysregulated social behavior [30]. In agreement with this, our data show that Lrig1-deficient mice exhibit hippocampal dendritic abnormalities that correlate with deficits in social paradigms. Because several neuropsychiatric disorders are associated with altered social phenotypes, our findings raise the possibility that Lrig1 dysfunction may contribute to these brain disorders. Thus, a more detailed behavioral characterization of Lrig1-mutant mice may provide a new target for therapeutic approaches to the treatment of social disorders.

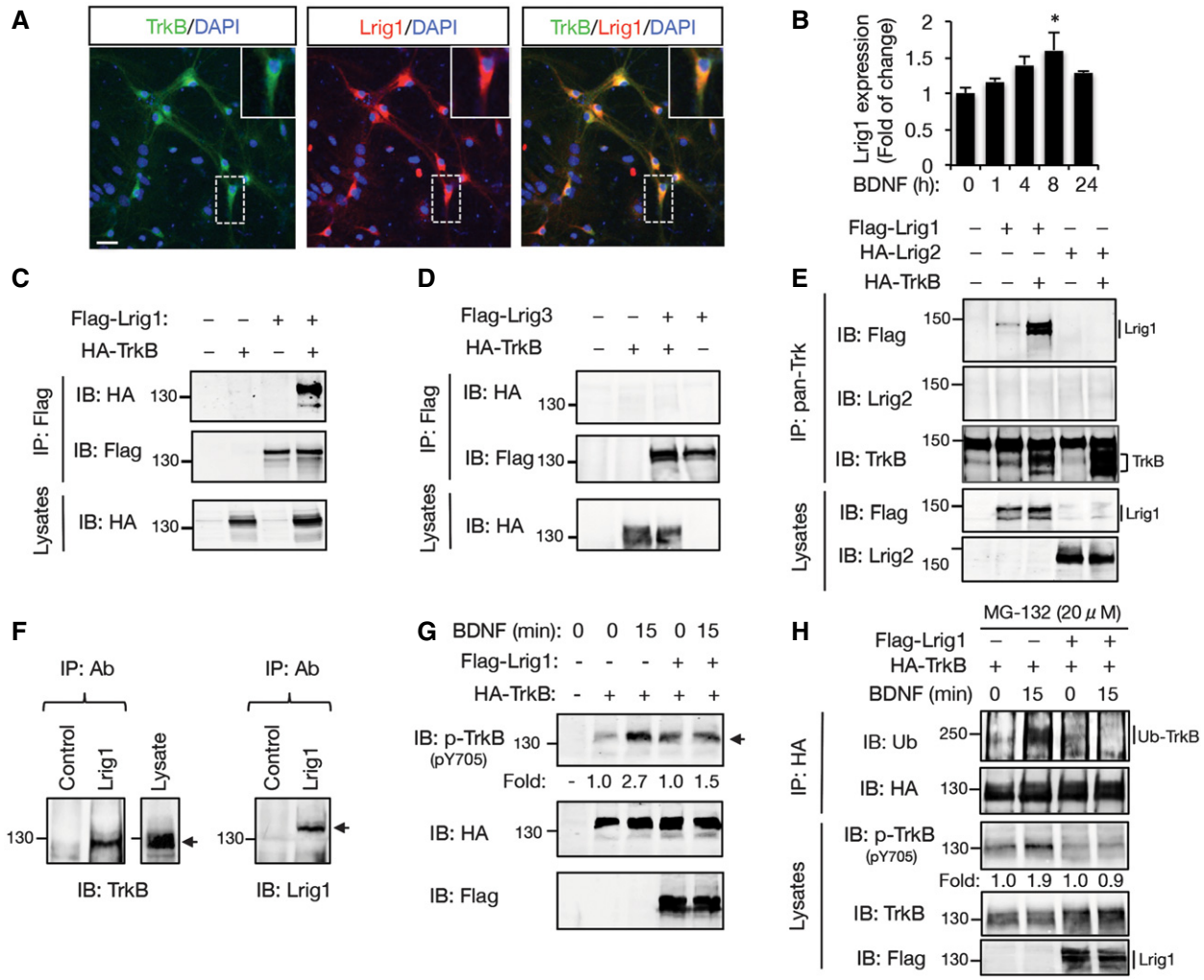

Figure 6. Lrig1 interacts with TrkB to abrogate receptor activation and its expression is induced in hippocampal neurons by BDNF.

A Coexpression of Lrig1 (red) and TrkB (green) in primary rat hippocampal neurons. Boxed area represents a higher magnification image showing a high colocalization between TrkB and Lrig1 in a pyramidal neuron. Yellow indicates regions of colocalization. Scale bar, 30 μm. Data represent $n = 3$ independent experiments.

B Quantitative analysis of *Lrig1* mRNA expression by real-time RT–PCR. Rat hippocampal cultures (10 DIV) were treated with BDNF (50 ng/ml) during the indicated times. The levels were normalized using the expression of the housekeeping gene *Tbp*. The results are shown as mean ± SD of $n = 3$ independent experiments. *$P < 0.05$ vs. control group by one-way ANOVA followed by Dunnett's test.

C, D Coimmunoprecipitation between Flag-Lrig1 and HA-TrkB (C) or between Flag-Lrig3 and HA-TrkB (D) overexpressed in HEK293 cells. Cell extracts were analyzed by immunoprecipitation with anti-Flag antibodies followed by immunoblot (IB) with antibodies against HA. Reprobing of the same blots with anti-Flag antibodies is shown below. The bottom panel shows HA expression in total lysates. Data represent $n = 3$ independent experiments.

E Coimmunoprecipitation between HA-TrkB and Flag-Lrig1 or between HA-TrkB and HA-Lrig2 exogenously expressed in HEK293 cells. Cell extracts were analyzed by IP with anti-pan-Trk antibodies followed by IB with antibodies against Flag or Lrig2. Reprobing of the same blots with anti-TrkB antibodies is shown below. The bottom panels show Flag and Lrig2 expression in total lysates. Data represent $n = 2$ independent assays.

F *In vivo* interaction between Lrig1 and TrkB. Coimmunoprecipitation between Lrig1 and TrkB receptor endogenously expressed from P15 rat hippocampal tissue extracts. Samples were equally divided into two parts, and then, the analysis was done by immunoprecipitation with control (anti-HA epitope tag antibody) or anti-Lrig1 antibodies, followed by immunoblotting with anti-TrkB antibody. Reprobing of the same blot with anti-Lrig1 antibody is also shown. Expression of TrkB in one aliquot of the starting material (indicated as lysate) is included. Arrow indicates the band of TrkB coimmunoprecipitated with anti-Lrig1 antibody. Similar results were obtained in $n = 3$ independent assays.

G Ligand-dependent activation of TrkB (p-TrkB) was evaluated by transient transfection of HA-TrkB plasmid with either a control or a Flag-Lrig1 vector into HEK cells. After 36 h, cells were serum-starved and stimulated with or without BDNF (30 ng/ml) for 15 min. The level of TrkB activation (p-TrkB) was evaluated in total cell lysates by immunoblotting (IB) with a specific antibody that recognizes TrkB phosphorylated in tyrosine 705 (pY705). Reprobing of the same blot with anti-HA and anti-Flag antibodies is shown. Fold of p-TrkB change relative to total TrkB is indicated. Similar results were obtained in $n = 3$ independent assays.

H TrkB ubiquitination was evaluated by transient transfection of HA-TrkB plasmid with either a control or a Flag-Lrig1 vector into MN1 cells. After 36 h, cells were serum-starved, pre-treated with the cell-permeable proteasome inhibitor MG-132 (20 μM), and stimulated with BDNF for 15 min. Total lysates were immunoprecipitated with anti-HA antibodies followed by immunoblot (IB) with antibodies against ubiquitin. Reprobing of the same blot with anti-HA antibodies is also shown. TrkB activation (p-TrkB) was evaluated in cell lysates. Reprobing of the same blot with anti-TrkB and anti-Flag antibodies is also shown. Fold of p-TrkB (p-Y705) change relative to total TrkB is indicated. Data represent $n = 3$ independent assays.

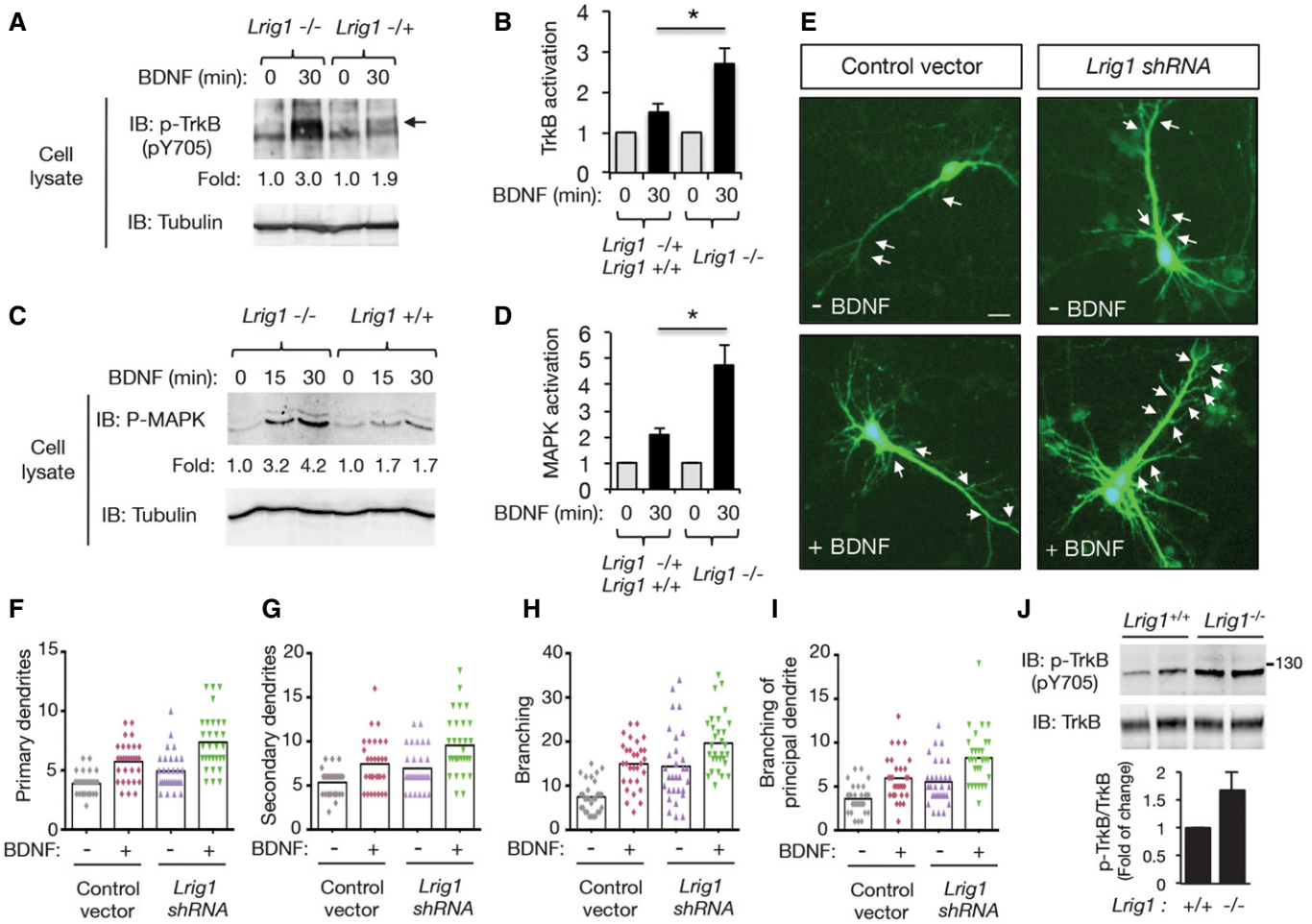

Figure 7. Lrig1 downregulation enhances TrkB signaling and dendrite development of primary hippocampal neurons in responses to BDNF.

A Immunoblot showing TrkB activation in hippocampal neurons cultured from Lrig1 heterozygous (+/−) and Lrig1 knockout (−/−) mice littermates treated in the absence or in the presence of BDNF (30 ng/ml) for 30 min. Reprobing of the same blot with anti-βIII-tubulin is shown as a loading control.

B Fold of TrkB activation relative to unstimulated control group (phospho-TrkB at Tyr705) in hippocampal neurons cultured from Lrig1 (+/+; +/−) and Lrig1 (−/−) mice treated in the absence or in the presence of BDNF (30 ng/ml) for 30 min. Results are presented as mean ± SEM of $n = 4$ independent experiments (*$P < 0.05$ by Student's t-test).

C Immunoblot showing MAPK activation in hippocampal neurons cultured from Lrig1 wild-type (+/+) and Lrig1-deficient (−/−) mice littermates treated in the absence or in the presence of BDNF (30 ng/ml) for the indicated times. Reprobing of the same blot with anti-βIII-tubulin is shown as a loading control. Fold of MAPK activation relative to tubulin is indicated.

D Fold of MAPK activation (P-MAPK) relative to untreated control group in hippocampal neurons cultured from Lrig1 (+/+; +/−) and Lrig1 (−/−) mice treated in the absence or in the presence of BDNF (30 ng/ml) for 30 min. Results are presented as mean ± SEM of $n = 4$ independent experiments (*$P < 0.05$ by Student's t-test).

E Representative images of mouse hippocampal neurons transfected at 4 DIV with either GFP-expressing control vector or *Lrig1*-shRNA-GFP plasmid. After transfection, neurons were cultured in the absence or in the presence of BDNF (25 ng/ml) for 48 h (7 DIV). Arrows indicate branching points along the principal dendrite. Scale bar, 10 μm.

F–I Quantification of primary dendrites (F), secondary dendrites (G), total branching (H), and branching of the principal dendrite (I) of hippocampal neurons treated as indicated in (E). The results are shown as individual values and the means of a representative assay. A total of 30 neurons were analyzed per experimental condition. Similar results were obtained in $n = 3$ independent experiments.

J *Lrig1*$^{+/+}$ and *Lrig1*$^{-/-}$ hippocampal lysates from postnatal day 11 (P11) mice were immunoblotted against phospho-TrkB (p-TrkB) at Tyr705 and total TrkB. Quantification (mean ± SD) of the p-TrkB/TrkB ratio between *Lrig1*$^{+/+}$ ($n = 4$) and *Lrig1*$^{-/-}$ ($n = 3$) hippocampi is also shown.

Although the view of Lrig function *in vivo* is far from complete, physiological evidence indicates that *Lrig* genes have redundant and independent functions during development. For instance, while loss of Lrig1 or Lrig2 impairs cochlear function, sensory innervation of the cochlea is only disrupted in *Lrig1/Lrig2* double-mutant mice [40]. Recently, it has been described that Lrig2 plays an important role in the control of cortical axon guidance and regeneration regulating ectodomain shedding of axon guidance receptors by ADAM proteases [41]. The functional contribution of Lrig3 during nervous system remains unknown.

LRR transmembrane proteins and nervous system development

Recent evidence indicates that LRR domain-containing transmembrane proteins have emerged as key molecules that control the wiring and specificity of the synaptic contacts, functioning as either

adhesion molecules or modulating neurotrophic growth factor receptor signaling during neural development [15,24,42].

Working *in trans* as cell adhesion molecules, many LRR transmembrane proteins affect axonal extension, guidance, target selection, and synapse formation [15,43–46]. Recent work has revealed the existence of multiple synaptic LRR proteins that influence when and where synapses are formed. Thus, functioning as trans-synaptic adhesion molecules, Slitrks, SALM, NGL, TrkC, and LRRTM proteins act at the time of the contact, providing positional information required during synapse formation. Surprisingly, the synaptogenic activity of TrkC, which is unique among the Trks, requires its LRR motif, but is independent of the NT3-binding domain [47]. This finding highlights a dual role of TrkC as a neurotrophin receptor and as a trans-synaptic adhesion molecule. Similarly, *Drosophila* Toll-like receptors utilize their LRR domains to function either as a repulsive cue to locally inhibit the innervation of motor neuron axons into the target tissue or as neurotrophin receptors [48].

On the other hand, other LRR transmembrane molecules such as Lrig1, Lingo1, Linx, and Slitrk5 have been characterized as cell type-specific modulators of neurotrophic growth factor signaling. In particular, these proteins physically interact with RTKs to attenuate or promote neurotrophic factor receptor signaling in spatially and temporally controlled manners, acting at specific points after receptor engagement [25,37,49]. It has been proposed that these regulatory proteins containing LRR domains may have evolved not only to avoid signaling errors that could lead to aberrant neuronal physiology but also to increase the repertoire of neurotrophic growth factor receptor signaling intensities and biological effects. Thus, these cell type-specific modulators allow us to understand how a limited number of neurotrophic factors and receptors can control the complexity of the neuronal connectivity and plasticity. Previous data suggest that Trk receptors may associate with LRR transmembrane proteins to control the outcome of Trk signaling. The LRR protein, Linx, was identified as a TrkA interactor able to increase TrkA signaling in developing sensory neurons and to facilitate NGF-induced axonal extension and target tissue innervation [42]. In addition, a recent study shows that another LRR-containing protein, Slitrk5, facilitates BDNF-induced TrkB signaling and biological responses to BDNF in GABAergic striatal neurons [49]. In contrast to these two LRR proteins, here we found that Lrig1 negatively regulates BDNF-induced TrkB signaling required to hippocampal dendrite development. In summary, all this evidence indicates that engagement of Trk receptors with different LRR domain-containing proteins is a new general mechanism of how specific populations of neurons expand the repertoire of neurotrophin signaling outputs during nervous system development.

LRR-containing proteins control RTK activity acting through different mechanisms such as receptor ubiquitination, ligand binding, and receptor trafficking. In particular, Lrig1 restricts ErbB and Met activities by enhancing receptor ubiquitination and degradation [21–23], and inhibits GDNF-induced Ret activation by a mechanism that involves inhibition of ligand binding and recruitment of Ret to lipid raft domains [24]. Our findings demonstrate that Lrig1 negatively controls TrkB activation in response to BDNF through a mechanism that does not involve receptor ubiquitination and degradation (Fig 6H). Although the molecular mechanism through which Lrig1 regulates TrkB signaling is still unknown, previous evidence obtained from different LRR transmembrane proteins suggests that Lrig1 could control TrkB activation acting at the level of BDNF binding and/or regulating TrkB trafficking.

TrkB signaling in dendrite morphogenesis and neuronal connectivity

Dendrite morphogenesis is a complex and exquisitely regulated process that includes the generation of dendritic branches that allow neurons to sculpt characteristic patterns of dendrite arborization and dendritic spines to connect among them. Increasing evidence indicates that a hallmark of a subgroup of cognitive and developmental disabilities is altered axonal and dendritic growth and branching [50]. Axonal and dendritic morphology is regulated by both growth-promoting and growth-inhibiting factors. BDNF and NT4 are neurotrophins that promote the development and plasticity of dendritic arbors and spines through TrkB receptor signaling [4,10,51,52].

Endocytosis and endosomal signaling is a crucial cellular mechanism that links neurotrophin-promoted Trk signaling to dendrite arborization [53]. Two recent studies identified two endosomal proteins (Rab11 and NHE6) involved in the control of TrkB signaling and required for neuronal circuit development [14,54].

During development, dendritic arbors adopt diverse branched morphologies of variable complexity that are characteristic for a given neuronal type. In particular, our data indicate that Lrig1 negatively regulates the dendritic morphology of hippocampal pyramidal neurons by attenuating neurotrophin receptor signaling. This newly discovered cell-autonomous role of Lrig1 in hippocampal development considerably expands the functions of this molecule for brain development, and represents a new way to regulate neurotrophin-induced effects in different areas of the vertebrate nervous system.

Materials and Methods

Recombinant proteins, reagents, and cell lines

COS-7 and HEK-293T cells were grown in Dulbecco's modified Eagle's medium (DMEM) supplemented with 10% fetal bovine serum (FBS) [24]. MN1 is an immortalized mouse-derived motor neuron cell line expressing Lrig1 that was cultured in DMEM supplemented with 7.5% FBS [24]. BDNF was purchased from R&D Systems (Abingdon, UK) and MG-132 was from Calbiochem.

Lrig1 RT–PCR

The expression of *Lrig1* and the expression of TATA box-binding protein (*Tbp*) mRNAs were analyzed. Total RNA was isolated from rat hippocampi at different embryonic and postnatal stages using RNA-easy columns (Qiagen). cDNA was synthesized using Multiscribe reverse transcriptase and random hexamers (Applied Biosystems). The cDNA was amplified using the following primer sets: *TATA box-binding protein (Tbp)*: forward, 5′-GGG GAG CTG TGA TGT GAA GT-3′; reverse, 5′- CCA GGA AAT AAT TCT GGC TCA-3′; *rat Lrig1:* forward, 5′-CTG CGT GTA AGG GAA CTC AAC-3′; reverse, 5′-GAT AGA CCA TCA AAC GCT CCA-3′.

Real-time PCR was performed using the SYBR Green qPCR SuperMix (Invitrogen) on an ABI7500 sequence detection system (Applied Biosystems), according to the manufacturer's instructions. Reactions were performed in 25 μl volume. Deoxynucleotides, Taq DNA polymerase, and buffer were included in the LightCycler-DNA master SYBR Green mix (Invitrogen).

Cell transfection and constructs

COS-7 and HEK-293T cells were transfected with Polyethylenimine-PEI (Polysciences). Hippocampal primary cultures were transfected with Lipofectamine 2000 (Invitrogen) in 300 μl of Neurobasal medium containing 1 μg of total plasmid DNA per well in 24-well plates. For downregulation experiments, hippocampal neurons were transfected with 1 μg of *Lrig1*-shRNA construct expressing GFP protein. For overexpression experiments, hippocampal neurons were cotransfected with Flag-tagged-Lrig1 (0.9 μg) construct and GFP expression vector (0.1 μg).

Lrig1-shRNA-GFP and HA-tagged Lrig2 constructs were purchased from Cellogenetics, Inc. The retroviral vector pRetro-U6G shRNA was used for expression of *Lrig1*-shRNA targeting mouse Lrig1 [24]. Plasmid cDNA encoding full-length Flag-tagged Lrig1 has been described previously [55]. A cDNA encoding flag-tagged mutated forms of Lrig1 lacking LRR and Ig-like domains (ΔLRRIg) and the LRR domains (ΔLRR) were kindly provided by Dr. Y. Yarden (Weizmann Institute, Israel) [21]. Plasmid encoding Flag-Lrig3 was kindly provided by Lisa Goodrich (Harvard Medical School, USA) [56]. cDNA encoding HA-tagged TrkB has been described previously [57]. Plasmid encoding GFP was obtained from Clontech.

shRNA-mediated knockdown assays

Mouse *Lrig1*-shRNA-GFP expression vector was purchased from Cellogenetics, Inc. The retroviral vector pRetro-U6G shRNA was used for expression of *Lrig1*-shRNA targeting mouse *Lrig1*. The target sequence of the *Lrig1*-shRNA is 5′-TCA GTC ACA TTG CTG AAG G-3′ and corresponds to nucleotides 1494–1512 of mouse *Lrig1 mRNA*. This region was not homologous to Lrig2, Lrig3, or other known genes determined by a BLAST search. The efficiency of mouse Lrig1 downregulation was confirmed by real-time PCR (Fig 2H), immunoblot, and immunofluorescence (Fig EV2).

Antibodies

The antibodies were obtained from various sources as follows: anti-phosphotyrosine (p-Tyr) and anti-phospho-TrkB (p-Tyr 705) were from Santa Cruz Biotechnology, anti-TrkB was from BD Biosciences Pharmingen, rabbit polyclonal anti-Lrig1 extracellular domain (gift from Dr. Satoshi Itami, University of Osaka, Osaka, Japan) [19,24], anti-Lrig1 intracellular domain was from R&D Systems, anti-HA was from Roche, rabbit polyclonal anti-Lrig2-147 [58] and rabbit polyclonal anti-Lrig3-207 were from Dr. Håkan Hedman laboratory (Umeå University, Sweden), anti-phospho-MAPK (Thr-202/Tyr-204) was from New England Biolabs, anti-βIII-tubulin was from Promega, anti-MAP-2, anti-S100β, and anti-Flag (M2) were from Sigma, and anti-ubiquitin was from Millipore.

Immunofluorescence and microscopy

Cryostat sections of postnatal day 15 (P15) brains were blocked with 10% donkey serum and incubated with rabbit polyclonal anti-Lrig1 extracellular domain (dilution 1/1,000). Dissociated hippocampal neurons obtained from E17.5 rat embryos and cultured by several days *in vitro* were fixed with 4% PFA, blocked with 10% donkey serum and then incubated with rabbit polyclonal anti-Lrig1 extracellular domain (gift from Dr. Satoshi Itami, 1/1,000) [19,59,60], anti-TrkB (1/200, BD Biosciences) [61], anti-MAP2 (1/1,000, Sigma), anti-S100β (1/1,000, Sigma), and anti-βIII-tubulin (1/5,000, Promega) antibodies. Secondary antibodies were from Jackson ImmunoResearch. Photographs were obtained using an Olympus IX-81 inverted microscope.

Lrig1-null mice

The *Lrig1*-mutant mice will be described in detail elsewhere (D. Linquist & H. Hedman, unpublished data). Briefly, *Lrig1* exon 1 was ablated through homologous and Cre-recombinase-mediated recombinations. All mice tested were littermate progeny of matings between heterozygous *Lrig1* KO mice; and purposely maintained on a mixed sv129/C57BL/6 genetic background to avoid artifactual phenotypes caused by mutations in inbred strains. Animal experiments were in accordance with the institutional animal care and ethics committee of the School of Medicine (CICUAL-UBA). Ethical permit number: 2776/2013.

Primary culture of hippocampal neurons

Rat (Sprague Dawley) hippocampal neurons from embryonic day (E) 17.5 were dissociated by trituration and cultured in Neurobasal medium (Gibco) supplemented with B27 (Gibco), penicillin, streptomycin, and Glutamax (Gibco) as described previously [62].

Mouse (C57BL/6) hippocampal neurons were prepared from postnatal day 0 (P0) newborn animals. Briefly, following digestion with 45 U of papain and 0.05% DNase in Hank's balanced salt solution at 37°C for 20 min, the reaction was stopped by adding DMEM 10% FBS. Then, the hippocampi were mechanically triturated and the dissociated neurons were seeded in 24-well plates coated with poly-D-lysine (10 μg/ml). Two hours later the medium was replaced by Neurobasal medium supplemented with B27 (Gibco), penicillin, streptomycin, and Glutamax (Gibco) as described previously [63]. For transfection of primary cultures, hippocampal neurons were seeded in 24-well dishes at a density of $1–1.3 \times 10^5$ cells per coverslip. Cultures were grown for different days *in vitro* before transfection.

Assessment of dendrite morphology and dendritic spine density

The axon was identified and excluded based on the absence of MAP-2 immunostaining. This staining was performed in low-density cultures of $4–5 \times 10^4$ hippocampal cells per 24-well dish. Pictures of dissociated neurons were acquired using an Olympus IX-81 microscope, and measurements of dendritic complexity were done in neuronal cells that displayed a pyramidal-shaped morphology bearing a thick main dendrite and several thin dendrites. Dendritic arbor

complexity was analyzed using the Sholl analysis plug-in of NeuronJ. We performed Sholl analysis with a 10 or 15 μm ring interval starting from the soma. Dendrites < 3 μm in length were not counted.

For dendritic spine density, images were obtained using an Olympus confocal FV1000 microscope, using a 60× objective. For dendritic spine assays, a Z series projection of each neuron was made. The number of spines on segments of at least 100 μm of dendritic length/neuron was counted.

Total cell lysates, immunoprecipitation, and Western blotting

Cells were lysed at 4°C in buffer containing 0.5% Triton X-100, 1% octyl-beta-glucoside plus protease and phosphatase inhibitors. Protein lysates were clarified by centrifugation and analyzed by immunoprecipitation and Western blotting as previously described [62]. The blots were scanned in a Storm 845 PhosphorImager (GE Healthcare Life Sciences), and quantifications were done with ImageQuant software (GE Healthcare Life Sciences). Numbers below the lanes indicate fold of induction relative to control normalized to total levels of the target protein.

Golgi staining

Briefly, mice brains were placed in fixative solution (formalin 10%) and stored in the darkness for 24 h at room temperature (RT). Then, the brains were transferred into a 3% potassium dichromate solution and stored at RT for 4 days. Thereafter, the brains were transferred into a 2% silver nitrate solution for 24 h. The brains were cut in sections of 100 μm thickness using a vibratome. Hippocampal sections were collected on a 0.3% gelatin solution, dried at room temperature, dehydrated in alcohol, and cleared with xylene. Finally, they were mounted on 0.3% gelatinized slides. Proximal complexity and branching (Sholl analysis) of apical and basal dendritic domains were evaluated in labeled hippocampal CA1 pyramidal neurons. Bright field images were taken on a Zeiss Axiophot microscope.

Social interaction and social novelty assays

We used an established three-chamber box test [64,65]. Briefly, the testing apparatus consisted of a clear Plexiglas rectangular box (60 × 40 × 22 cm) with three interconnected chambers, placed under dim light (25 lux). The apparatus was covered with clean bedding. Testing consisted of three 10-min sessions. In the first habituation session, subject mice (4–5 weeks old) were allowed to freely investigate the three-chamber box. This session was followed by a sociability session of 10 min, where the subject encounters a caged never-before-met mouse (stranger 1) and one empty container (non-social stimuli) in the opposite side of the apparatus. The location of the stranger mouse was alternated from left to right across subject testing. Then, in the social novelty session, a second novel mouse (stranger 2) was placed under the previous empty container. Thus, in the novelty session, the subject has to encounter the first intruder (stranger 1) as well as a second never-before-met intruder (stranger 2) under another container. The time spent sniffing the social (stranger1) and non-social stimuli (social interaction test) and the time spent sniffing the familiar vs. novel intruder mice caged in each chamber (social novelty) were measured. All sessions were video recorded through a camera mounted above the testing box.

Statistics

Data are reported as mean ± SEM or SD as indicated, and significance was accepted at $P < 0.05$. No statistical method was used to predetermine sample sizes, but our sample sizes are similar to those generally used in the field. The selection of the mice was unbiased in terms of size and weight. For animal studies, the handling of the data was performed in a blinded manner. Experiments were considered as independent when done from distinct litters. Statistical analysis was performed in GraphPad Prism 5.0. Normality of the data was evaluated with the Kolmogorov–Smirnov test. In the indicated cases, Student's *t*-test or ANOVA was performed.

Expanded View for this article is available online.

Acknowledgements

We thank Dr. Marcal Vilar, Dr. Alejandro Schinder, and Dr. Helena Mira for comments on the manuscript; Dr. Tomás Falzone for experimental assistance; A. Pecile and M. Ponce for animal care, Roux-Ocefa for reagent supply, and Innova-T and UBATEC for research grant administration. This work was supported by the Argentine Agency for Promotion of Science and Technology (ANPCyT) PICT2010-1012, PICT2013-0914, and UBACyT-2013-2016-GC (20020120100026BA). GP and FL were supported by an Independent Research Career Position from the Argentine Medical Research Council (CONICET). FCA, FH, DI, and PF were supported by a fellowship from CONICET.

Author contributions

FCA, FJH, FL, and GP conceived and designed the experiments. FCA, FJH, PAF, and DI performed the experiments and statistical analysis. FCA, FJH, FL, and GP helped in analysis and interpretation of the data. HH provided a new strain of Lrig1-knockout mice and gave scientific advice. GP wrote the manuscript.

Conflict of interest

The authors declare that they have no conflict of interest.

References

1. Parrish JZ, Emoto K, Kim MD, Jan YN (2007) Mechanisms that regulate establishment, maintenance, and remodeling of dendritic fields. *Annu Rev Neurosci* 30: 399 – 423
2. Wong RO, Ghosh A (2002) Activity-dependent regulation of dendritic growth and patterning. *Nat Rev Neurosci* 3: 803 – 812
3. Whitford KL, Dijkhuizen P, Polleux F, Ghosh A (2002) Molecular control of cortical dendrite development. *Annu Rev Neurosci* 25: 127 – 149
4. Reichardt LF (2006) Neurotrophin-regulated signalling pathways. *Philos Trans R Soc Lond B Biol Sci* 361: 1545 – 1564
5. Segal RA, Pomeroy SL, Stiles CD (1995) Axonal growth and fasciculation linked to differential expression of BDNF and NT3 receptors in developing cerebellar granule cells. *J Neurosci* 15: 4970 – 4981
6. McAllister AK, Katz LC, Lo DC (1996) Neurotrophin regulation of cortical dendritic growth requires activity. *Neuron* 17: 1057 – 1064
7. Horch HW, Kruttgen A, Portbury SD, Katz LC (1999) Destabilization of cortical dendrites and spines by BDNF. *Neuron* 23: 353 – 364

8. Jin X, Hu H, Mathers PH, Agmon A (2003) Brain-derived neurotrophic factor mediates activity-dependent dendritic growth in nonpyramidal neocortical interneurons in developing organotypic cultures. *J Neurosci* 23: 5662 – 5673
9. Ji Y, Lu Y, Yang F, Shen W, Tang TT, Feng L, Duan S, Lu B (2010) Acute and gradual increases in BDNF concentration elicit distinct signaling and functions in neurons. *Nat Neurosci* 13: 302 – 309
10. Greenberg ME, Xu B, Lu B, Hempstead BL (2009) New insights in the biology of BDNF synthesis and release: implications in CNS function. *J Neurosci* 29: 12764 – 12767
11. McAllister AK, Lo DC, Katz LC (1995) Neurotrophins regulate dendritic growth in developing visual cortex. *Neuron* 15: 791 – 803
12. Cheung ZH, Chin WH, Chen Y, Ng YP, Ip NY (2007) Cdk5 is involved in BDNF-stimulated dendritic growth in hippocampal neurons. *PLoS Biol* 5: e63
13. Kwon M, Fernandez JR, Zegarek GF, Lo SB, Firestein BL (2011) BDNF-promoted increases in proximal dendrites occur via CREB-dependent transcriptional regulation of cypin. *J Neurosci* 31: 9735 – 9745
14. Lazo OM, Gonzalez A, Ascano M, Kuruvilla R, Couve A, Bronfman FC (2013) BDNF regulates Rab11-mediated recycling endosome dynamics to induce dendritic branching. *J Neurosci* 33: 6112 – 6122
15. de Wit J, Hong W, Luo L, Ghosh A (2011) Role of leucine-rich repeat proteins in the development and function of neural circuits. *Annu Rev Cell Dev Biol* 27: 697 – 729
16. Proenca CC, Gao KP, Shmelkov SV, Rafii S, Lee FS (2011) Slitrks as emerging candidate genes involved in neuropsychiatric disorders. *Trends Neurosci* 34: 143 – 153
17. Chen Y, Hor HH, Tang BL (2012) AMIGO is expressed in multiple brain cell types and may regulate dendritic growth and neuronal survival. *J Cell Physiol* 227: 2217 – 2229
18. de Wit J, Ghosh A (2014) Control of neural circuit formation by leucine-rich repeat proteins. *Trends Neurosci* 37: 539 – 550
19. Suzuki Y, Miura H, Tanemura A, Kobayashi K, Kondoh G, Sano S, Ozawa K, Inui S, Nakata A, Takagi T *et al* (2002) Targeted disruption of LIG-1 gene results in psoriasiform epidermal hyperplasia. *FEBS Lett* 521: 67 – 71
20. Nilsson J, Vallbo C, Guo D, Golovleva I, Hallberg B, Henriksson R, Hedman H (2001) Cloning, characterization, and expression of human LIG1. *Biochem Biophys Res Commun* 284: 1155 – 1161
21. Gur G, Rubin C, Katz M, Amit I, Citri A, Nilsson J, Amariglio N, Henriksson R, Rechavi G, Hedman H *et al* (2004) LRIG1 restricts growth factor signaling by enhancing receptor ubiquitylation and degradation. *EMBO J* 23: 3270 – 3281
22. Laederich MB, Funes-Duran M, Yen L, Ingalla E, Wu X, Carraway KL 3rd, Sweeney C (2004) The leucine-rich repeat protein LRIG1 is a negative regulator of ErbB family receptor tyrosine kinases. *J Biol Chem* 279: 47050 – 47056
23. Shattuck DL, Miller JK, Laederich M, Funes M, Petersen H, Carraway KL 3rd, Sweeney C (2007) LRIG1 is a novel negative regulator of the Met receptor and opposes Met and Her2 synergy. *Mol Cell Biol* 27: 1934 – 1946
24. Ledda F, Bieraugel O, Fard SS, Vilar M, Paratcha G (2008) Lrig1 is an endogenous inhibitor of Ret receptor tyrosine kinase activation, downstream signaling, and biological responses to GDNF. *J Neurosci* 28: 39 – 49
25. Alsina FC, Ledda F, Paratcha G (2012) New insights into the control of neurotrophic growth factor receptor signaling: implications for nervous system development and repair. *J Neurochem* 123: 652 – 661
26. Kwon CH, Luikart BW, Powell CM, Zhou J, Matheny SA, Zhang W, Li Y, Baker SJ, Parada LF (2006) Pten regulates neuronal arborization and social interaction in mice. *Neuron* 50: 377 – 388
27. Sholl A, Uttley AM (1953) Pattern discrimination and the visual cortex. *Nature* 171: 387 – 388
28. Kaufmann WE, Moser HW (2000) Dendritic anomalies in disorders associated with mental retardation. *Cereb Cortex* 10: 981 – 991
29. Penzes P, Woolfrey KM, Srivastava DP (2011) Epac2-mediated dendritic spine remodeling: implications for disease. *Mol Cell Neurosci* 46: 368 – 380
30. Jan YN, Jan LY (2010) Branching out: mechanisms of dendritic arborization. *Nat Rev Neurosci* 11: 316 – 328
31. Felix-Ortiz AC, Tye KM (2014) Amygdala inputs to the ventral hippocampus bidirectionally modulate social behavior. *J Neurosci* 34: 586 – 595
32. Phelps SM, Campbell P, Zheng DJ, Ophir AG (2010) Beating the boojum: comparative approaches to the neurobiology of social behavior. *Neuropharmacology* 58: 17 – 28
33. Nibuya M, Morinobu S, Duman RS (1995) Regulation of BDNF and trkB mRNA in rat brain by chronic electroconvulsive seizure and antidepressant drug treatments. *J Neurosci* 15: 7539 – 7547
34. Tongiorgi E, Righi M, Cattaneo A (1997) Activity-dependent dendritic targeting of BDNF and TrkB mRNAs in hippocampal neurons. *J Neurosci* 17: 9492 – 9505
35. Drake CT, Milner TA, Patterson SL (1999) Ultrastructural localization of full-length trkB immunoreactivity in rat hippocampus suggests multiple roles in modulating activity-dependent synaptic plasticity. *J Neurosci* 19: 8009 – 8026
36. Elmariah SB, Crumling MA, Parsons TD, Balice-Gordon RJ (2004) Postsynaptic TrkB-mediated signaling modulates excitatory and inhibitory neurotransmitter receptor clustering at hippocampal synapses. *J Neurosci* 24: 2380 – 2393
37. Ledda F, Paratcha G (2007) Negative regulation of receptor tyrosine kinase (RTK) signaling: a developing field. *Biomarker Insights* 2: 45 – 58
38. Dikic I, Giordano S (2003) Negative receptor signalling. *Curr Opin Cell Biol* 15: 128 – 135
39. Puram SV, Bonni A (2013) Cell-intrinsic drivers of dendrite morphogenesis. *Development* 140: 4657 – 4671
40. Del Rio T, Nishitani AM, Yu WM, Goodrich LV (2013) In vivo analysis of Lrig genes reveals redundant and independent functions in the inner ear. *PLoS Genet* 9: e1003824
41. van Erp S, van den Heuvel DM, Fujita Y, Robinson RA, Hellemons AJ, Adolfs Y, Van Battum EY, Blokhuis AM, Kuijpers M, Demmers JA *et al* (2015) Lrig2 negatively regulates ectodomain shedding of axon guidance receptors by ADAM proteases. *Dev Cell* 35: 537 – 552
42. Mandai K, Guo T, St Hillaire C, Meabon JS, Kanning KC, Bothwell M, Ginty DD (2009) LIG family receptor tyrosine kinase-associated proteins modulate growth factor signals during neural development. *Neuron* 63: 614 – 627
43. de Wit J, Sylwestrak E, O'Sullivan ML, Otto S, Tiglio K, Savas JN, Yates JR 3rd, Comoletti D, Taylor P, Ghosh A (2009) LRRTM2 interacts with Neurexin1 and regulates excitatory synapse formation. *Neuron* 64: 799 – 806
44. Takahashi H, Katayama K, Sohya K, Miyamoto H, Prasad T, Matsumoto Y, Ota M, Yasuda H, Tsumoto T, Aruga J *et al* (2012) Selective control of inhibitory synapse development by Slitrk3-PTPdelta trans-synaptic interaction. *Nat Neurosci* 15(389–398): S381 – S382
45. Linhoff MW, Lauren J, Cassidy RM, Dobie FA, Takahashi H, Nygaard HB, Airaksinen MS, Strittmatter SM, Craig AM (2009) An unbiased expression

screen for synaptogenic proteins identifies the LRRTM protein family as synaptic organizers. *Neuron* 61: 734 – 749

46. Nam J, Mah W, Kim E (2011) The SALM/Lrfn family of leucine-rich repeat-containing cell adhesion molecules. *Semin Cell Dev Biol* 22: 492 – 498
47. Takahashi H, Arstikaitis P, Prasad T, Bartlett TE, Wang YT, Murphy TH, Craig AM (2011) Postsynaptic TrkC and presynaptic PTPsigma function as a bidirectional excitatory synaptic organizing complex. *Neuron* 69: 287 – 303
48. McIlroy G, Foldi I, Aurikko J, Wentzell JS, Lim MA, Fenton JC, Gay NJ, Hidalgo A (2013) Toll-6 and Toll-7 function as neurotrophin receptors in the *Drosophila* melanogaster CNS. *Nat Neurosci* 16: 1248 – 1256
49. Song M, Giza J, Proenca CC, Jing D, Elliott M, Dincheva I, Shmelkov SV, Kim J, Schreiner R, Huang SH *et al* (2015) Slitrk5 mediates BDNF-dependent TrkB receptor trafficking and signaling. *Dev Cell* 33: 690 – 702
50. Kulkarni VA, Firestein BL (2012) The dendritic tree and brain disorders. *Mol Cell Neurosci* 50: 10 – 20
51. Cohen S, Greenberg ME (2008) Communication between the synapse and the nucleus in neuronal development, plasticity, and disease. *Annu Rev Cell Dev Biol* 24: 183 – 209
52. Yang J, Harte-Hargrove LC, Siao CJ, Marinic T, Clarke R, Ma Q, Jing D, Lafrancois JJ, Bath KG, Mark W *et al* (2014) proBDNF negatively regulates neuronal remodeling, synaptic transmission, and synaptic plasticity in hippocampus. *Cell Rep* 7: 796 – 806
53. Cosker KE, Segal RA (2014) Neuronal signaling through endocytosis. *Cold Spring Harb Perspect Biol* 6: a020669
54. Ouyang Q, Lizarraga SB, Schmidt M, Yang U, Gong J, Ellisor D, Kauer JA, Morrow EM (2013) Christianson syndrome protein NHE6 modulates TrkB endosomal signaling required for neuronal circuit development. *Neuron* 80: 97 – 112
55. Nilsson J, Starefeldt A, Henriksson R, Hedman H (2003) LRIG1 protein in human cells and tissues. *Cell Tissue Res* 312: 65 – 71
56. Abraira VE, Satoh T, Fekete DM, Goodrich LV (2010) Vertebrate Lrig3-ErbB interactions occur in vitro but are unlikely to play a role in Lrig3-dependent inner ear morphogenesis. *PLoS ONE* 5: e8981
57. Bibel M, Hoppe E, Barde YA (1999) Biochemical and functional interactions between the neurotrophin receptors trk and p75NTR. *EMBO J* 18: 616 – 622
58. Rondahl V, Holmlund C, Karlsson T, Wang B, Faraz M, Henriksson R, Hedman H (2013) Lrig2-deficient mice are protected against PDGFB-induced glioma. *PLoS ONE* 8: e73635
59. Jensen KB, Watt FM (2006) Single-cell expression profiling of human epidermal stem and transit-amplifying cells: Lrig1 is a regulator of stem cell quiescence. *Proc Natl Acad Sci USA* 103: 11958 – 11963
60. Nakamura T, Hamuro J, Takaishi M, Simmons S, Maruyama K, Zaffalon A, Bentley AJ, Kawasaki S, Nagata-Takaoka M, Fullwood NJ *et al* (2014) LRIG1 inhibits STAT3-dependent inflammation to maintain corneal homeostasis. *J Clin Invest* 124: 385 – 397
61. Berghuis P, Dobszay MB, Wang X, Spano S, Ledda F, Sousa KM, Schulte G, Ernfors P, Mackie K, Paratcha G *et al* (2005) Endocannabinoids regulate interneuron migration and morphogenesis by transactivating the TrkB receptor. *Proc Natl Acad Sci USA* 102: 19115 – 19120
62. Paratcha G, Ledda F, Ibanez CF (2003) The neural cell adhesion molecule NCAM is an alternative signaling receptor for GDNF family ligands. *Cell* 113: 867 – 879
63. Otero MG, Alloatti M, Cromberg LE, Almenar-Queralt A, Encalada SE, Pozo Devoto VM, Bruno L, Goldstein LS, Falzone TL (2014) Fast axonal transport of the proteasome complex depends on membrane interaction and molecular motor function. *J Cell Sci* 127: 1537 – 1549
64. Alfieri JA, Pino NS, Igaz LM (2014) Reversible behavioral phenotypes in a conditional mouse model of TDP-43 proteinopathies. *J Neurosci* 34: 15244 – 15259
65. Nadler JJ, Moy SS, Dold G, Trang D, Simmons N, Perez A, Young NB, Barbaro RP, Piven J, Magnuson TR *et al* (2004) Automated apparatus for quantitation of social approach behaviors in mice. *Genes Brain Behav* 3: 303 – 314

